INTERNATIONAL JOURNAL OF RIVER BASIN MANAGEMENT
https://doi.org/10.1080/15715124.2023.2294449

Taylor & Francis
Taylor & Francis Group

RESEARCH ARTICLE

A comparison of Eulerian and semi-Lagrangian approaches for modeling stream water quality

A. Sulis[a], T.B. Wild[b,c,d] and D.P. Loucks[e]

[a]Department of Architecture, Design and Urban planning (DADU), University of Sassari, Alghero, Italy; [b]Joint Global Change Research Institute, Pacific Northwest National Laboratory, College Park, MD, USA; [c]Earth System Science Interdisciplinary Center (ESSIC), University of Maryland, College Park, MD, USA; [d]Department of Civil and Environmental Engineering, University of Maryland, College Park, MD, USA; [e]School of Civil and Environmental Engineering, Cornell University, Ithaca, NY, USA

ABSTRACT

This paper describes and compares some of the advantages and limitations of Eulerian and Lagrangian approaches to water quality modeling and introduces a mixed Eulerian-Lagrangian (or semi-Lagrangian) methodology that captures the strengths of both approaches. The semi-Lagrangian modeling approach is applied to advection-dominated rivers, and flexibly ensures unconditional stability for all time step durations and grid segmentations. The semi-Lagrangian modeling approach is demonstrated by applying it to estimate the dissolved oxygen concentrations in the Sava River in Slovenia, focusing on aspects of the methodology and findings that would be of broad interest to managers of water quality in fluvial water bodies. Results of comparisons of the semi-Lagrangian model with the Eulerian-based QUAL2K model in steady and non-steady scenarios demonstrate that while both models are fully capable of producing satisfactory results when optimally configured, the semi-Lagrangian approach offers accuracy and stability without sensitivity to the interaction of time step size and computational grid segmentation scheme.

ARTICLE HISTORY
Received 13 May 2023
Accepted 10 December 2023

ASSOCIATE EDITOR
Michael Nones

KEYWORDS
Water quality management; *semi-Lagrangian modeling*; advection–diffusion; stream water quality model software; dissolved oxygen concentrations; *Sava River*

Nomenclature

A	cross section area
B	parameter of energy dissipation model
BOD	Biochemical oxygen demand
C	constituent concentration
E_x	longitudinal dispersion coefficient
F	constituent flux
I	incremental flow to reach
k	temperature-dependent constant
k_a	reaeration rate constant
k_d	degradation rate constant for BOD
L_{ij}	distance from node i to node j
n	number of computational cells
Q:	flow rate
S	reach storage volume
SOD	sediment oxygen demand rate
T	Temperature of river water
Δt	time interval of simulation
h	surface elevation change
v	flow mean velocity
τ_{ij}	time of flow from node i to node j

1. Introduction

While science and policy advances have led to improved water quality in some parts of the world over the past several decades (e.g. Water Framework Directive WFD, 2000/60/CE in the European Union or the Water Quality Act of 1987, in the United States), globally nearly 70% of the world's riverine systems are still experiencing impaired water quality. Better understanding, and identifying potential solutions to, water quality challenges in these regions is central to meeting many of the Sustainable Development Goals (Alcamo 2019; Ho *et al.* 2020; Quinlivan *et al.* 2020; Tsani *et al.* 2020; Mraz *et al.* 2021). Exploring these challenges and opportunities will be particularly important as a growing global economy and a changing climate are poised to further stress river systems in the coming decades by increasing riverine waste loads and temperatures, and reducing dissolved oxygen concentrations (UNESCO 2020). Mathematical models of water quality processes are useful tools for scientists and engineers in identifying and evaluating alternative water management options that may impact water quality (Thomann and Mueller 1987; Chapra 1997; McIntosh *et al.* 2011). There have historically been two general approaches to water quality simulation: Eulerian and Lagrangian. In this paper we describe some of the advantages and disadvantages of these two approaches; introduce a mixed Eulerian-Lagrangian (or semi-Lagrangian) methodology that combines the two approaches; and demonstrate the utility of this combined approach in a real water quality setting in the Sava River in Slovenia, focusing on aspects of our methodology and findings that would be of broad interest in other river water quality studies.

The Eulerian approach has been the most widely used by water quality modelers. Aside from the common simulation of the convective transport of constituents in a river, examples of recent Eulerian applications in water ecosystems include river oil spills (Kvočka *et al.* 2021), toxic cyanobacteria movement (Ndong *et al.* 2017), movement of porpoises or other aquatic species (Fang *et al.* 2016), artificial radionuclide releases within a river (Duffa *et al.* 2016), coastal sediment transport (Cheng *et al.* 2017), and particle-laden flows (Zakharov and Bansmer 2021). Examples of widely-used models that implement methodologies characterized as Eulerian currently include MIKE11 (Danish Hydraulics

CONTACT A. Sulis asulis@uniss.it
Supplemental data for this article can be accessed online at https://doi.org/10.1080/15715124.2023.2294449.

Institute 2007), Qual2E (Q2E) (Brown and Barnwell 1987) and QUAL2K (QUAL2K) (Chapra *et al.* 2008), ISIS (Sir William Halcrow and Partners Ltd. and HR Wallingford 2002) and WASP 7 (Ambrose and Wool 2009).

Most large river systems globally are advection-dominated, rather than dispersion-dominated. (The latter occurs in systems such as estuaries or low-lying streams that are significantly influenced by tidal patterns). To increase the predictive accuracy of Eulerian models in advection-dominated settings requires increasing the grid segmentation (i.e. creating more grid cells in each river reach). However, this requires the use of smaller time steps to avoid numerical instability issues such as spurious oscillation, numerical dispersion, grid orientation, phase error, peak clipping, and valley elevating (Yeh *et al.* 1992; Manson and Wallis 2000) that have historically posed challenges for Eulerian models. Reducing the simulation time step increases computational time and expense (Manson and Wallis 2000). While this may not be a problem in studies of small systems with relatively few objectives, it poses a substantial challenge for studies of large river systems with multiple objectives (of which water quality may be just one) (Yosefipoor *et al.* 2022). Thus, in each study setting, there exist tradeoffs among accuracy, stability, and computational time that modelers must navigate.

The Lagrangian approach to water quality modeling tracks individual constituent mass particles in space and time with a continuously deforming global coordinate system, rather than creating a computational grid and focusing on a mass balance for each computational cell within each discrete time-step, as the Eulerian approach does. However, this approach can become difficult to implement and can be computationally expensive due to the lack of a convenient, fixed computational grid (Jobson 1981). Lagrangian water quality models are much less common than Eulerian models, but examples of implementation do exist (e.g. the Branched Lagrangian Transport Model (Jobson and Schoelhammer 1987)).

A third approach, often referred to in the literature as Eulerian-Lagrangian, or semi-Lagrangian (SL), combines the two traditional approaches (Eulerian and Lagrangian) into a hybrid approach that offers some advantages from both methodologies (Holly and Preissmann 1977; Oliviera and Baptista 1995). The semi-Lagrangian approach still requires a fixed computational grid, which comprises the Eulerian component of the methodology, but also includes a Lagrangian component that tracks each advected species along its fluid trajectory (or characteristic line). This approach results in well-documented improvements in efficiency and accuracy for advection-dominated systems, and flexibly ensures unconditional stability for all combinations of time step duration and grid segmentation. These are important benefits for modelers interested in simulating large space–time scale, complex riverine systems (Cheng *et al.* 1984; Yeh 1990; Zhang *et al.* 1993; Manson and Wallis 2000). While SL methods offer the possibility of large time step durations without loss in accuracy and/or without significant increase in computational expense, the methods have the following drawbacks: (1) potential non-conservation of mass; (2) a 'backtracking' step that can require computationally intensive (and thus time-consuming) numerical integration in non-steady state simulations; and (3) numerical dispersion or accuracy error that results from a temporal or spatial interpolation step (Wild 2011; Wild and Loucks 2012).

Examples of applications of the SL approach in water quality modeling are, in comparison to Eulerian implementations, recent and relatively uncommon (Manson *et al.* 2010; Wang *et al.* 2011; Cimorelli *et al.* 2016; Puigferrat *et al.* 2021). Fletcher (2020) presents a state-of-the-art summary of applications of SL methods in the large field of geosciences. Applications of SL methods may be relatively less common, in comparison to the Eulerian approach, because their clear advantages only become significant in larger space–time scale applications (Wild 2011; Wild and Loucks 2012). Riverine water quality modeling applications have traditionally been basin or sub-basin scale investigations, which have temporal and spatial scales that are less likely to benefit from the semi-Lagrangian approach (Yearsley 2009). However, the space–time scales of water quality modeling applications are becoming, and will continue to become, much larger and much more complex, which should make semi-Lagrangian models more appealing (Yearsley 2009). Additionally, water quality modeling software is increasingly being required to offer stochastic simulation capabilities (Neelz and Wallis 2007) that can be computationally intensive. SL models offer an approach in which such simulations can take place with more computational efficiency.

The potential improvements in numerical stability, accuracy, and computational time of semi-Lagrangian methods have been well documented in the literature (Yeh 1990; Ruan and McLaughlin, 1999; Young *et al.* 2000). However, few publications have focused on the theoretical development and application of user-friendly, surface water quality semi-Lagrangian models. Similarly, comparisons of Eulerian and semi-Lagrangian models in the literature are sparse. Of the semi-Lagrangian water quality models that have been developed (e.g. the DISCUS model by Manson and Wallis 2000), few are distributed with a user-friendly interface, and still fewer are built for those interested in simulating advection-dominated flow and transport of a large suite of specific water quality constituents in a complex stream network. This paper aims to help fill this void by (1) presenting the development and application of such a semi-Lagrangian model, the Stream Water Quality Model (SWQ); and (2) conducting a direct, multi-constituent comparison of this model with a widely used Eulerian model, QUAL2K (Chapra *et al.* 2008), to demonstrate that SWQ could serve as a quick, simple, and reliable alternative to QUAL2K in some applications.

2. SWQ model development

The original version of the SWQ model was developed by Sulis and Loucks (2007) to provide modelers with a simple, user-friendly, quick and accurate semi-Lagrangian water quality decision support tool. SWQ deterministically and one-dimensionally simulates flow and transport for a small suite of constituents for advection-dominated streams. For SWQ to be an attractive water quality screening model, the model was expanded by Wild (2011) to include more constituents and more complex constituent kinetic processes, which naturally resulted in the implementation of numerical techniques to solve the new and more complex differential equations. One goal of developing SWQ was to provide modelers with a screening option that is relatively simple

to use and that does not require the same extent of parameter estimation and data input as other 1-D water quality models. Another goal of developing SWQ was to provide the water quality modeling community with a tool capable of avoiding some of the complications that typically characterize Eulerian water quality models. For example, SWQ provides unconditionally stable and high-accuracy results for a variety of combinations of simulation time step durations and segmenting schemes, which provides flexibility for a wide range of potential water quality modeling applications. The model would be expected to perform particularly well, in comparison to Eulerian models, for simulations of systems requiring large time step durations, simulations of spatially extensive and/or complex (e.g. branched) stream networks with changing flow and loading conditions, simulations being performed as part of a computationally expensive optimization/calibration process, and simulations that are being performed only as a sub-component of another model.

2.1. Semi-Lagrangian approach in SWQ

2.1.1 Backtracking approach in SWQ

The SWQ model represents a stream system as a network consisting of nodes and arcs (i.e. links). Arcs are the river or stream segments between an upstream node '*i*' and a downstream node '*j*' having homogeneous hydraulic characteristics. Each stream segment is assumed to be in a steady-state condition during each simulation time step, but those steady-state conditions can change from one model time step to the next. Nodes can represent demand sites and/or incremental inflow sites (such as node *j* in Figure 1), or diversions and/or confluences.

At each simulation time step, the basic equations for hydrological models are solved. These include the continuity equation and the storage function in each reach (arc) *ij* connecting nodes *i* and *j*. The continuity equation defines the change in reach storage volume (dS_{ij}/dt) over time, as the difference between the reach inflow (Q_{ij}^{IN}) and the reach outflow (Q_{ij}^{OUT}):

$$Q_{ij}^{IN} - Q_{ij}^{OUT} = \frac{dS_{ij}}{dt} \tag{1}$$

Integrating this equation over a simulation time period yields the change in storage over the time period, as well as the total inflow and outflow volumes in the period. The SWQ model keeps track of the beginning and the ending storage volumes in each reach in each period *t*. The initial storage volume in the reach extending from node *i* to node *j* is designated as $S_{ij}(t)$. While in fact the outflow will change over the period as the reach storage volume changes, this model computes the total outflow in a period, Q_{ij}^{OUT}, and assumes the outflow rate, expressed as cubic meters per second, is constant over the period. Storage volumes are expressed in cubic meters. The total inflow rate at each node *j* during a simulation time period *t*, is the sum of all the outflows from entering arcs or links plus any incremental flow, $I_j(t)$:

$$Q_j^{IN}(t) = \sum_{i \quad connected \quad to \quad j} Q_{ij}^{OUT}(t) + I_j(t) \tag{2}$$

Continuity at each node requires the inflow to equal the outflow. If multiple outflowing links exist from node *j* to various nodes *k*, the user must define the fraction r_{jk} of total outflow that goes to each outflowing link *jk*. These fractions must obviously sum to 1. The user can select the most appropriate discharge equation to calculate the mean velocity v_{ij} as a function (analytical or semi-empirical) of Q_{ij}^{OUT} in each reach *j* during time period *t*.

Therefore, the time that it takes flow starting at node *i* to arrive at node *j*, over a distance L_{ij} [m] can be expressed as follows:

$$\tau_{ij}(t) = \frac{L_{ij}}{v_{ij}(t)} \tag{3}$$

In a traditional Eulerian approach, the nature of the grid segmentation dictates the maximum simulation time step that is possible without creating numerical stability issues. The SWQ model borrows the convenient Eulerian approach of creating a fixed grid on which calculations are performed but avoids this problematic maximum time step constraint (the so-called 'Courant condition'). As a result, SWQ users can conduct a simulation of any time step (e.g. 1 h or 1 week) coupled with any segmenting scheme (i.e. any number of computational elements of any size), without encountering numerical stability issues. In other words, the model preserves numerical integrity with larger time intervals than those required to meet the Courant conditions associated with Eulerian modeling approaches.

The Courant condition that creates challenges for the Eulerian methodology, but that is completely avoided by methodologies with Lagrangian elements, bears more discussion. The Eulerian approach, whether implicit or explicit in implementation (Natarajan and Jacobs 2020), can create numerical instability and accuracy deficiency in advection-dominated systems if the Courant condition is violated (Casulli and Cheng 1990). This condition is violated if, during a given simulation time step, the velocity of streamflow is sufficiently large that the flow from one stream or river segment passes through the immediately adjacent segment(s) and into the following segments. For example, in a 1-dimensional pure advection system composed by a series of *i* segments of length Δx_i, cross section area A_i and average flow Q_{it} in period *t*, the constraint is given by the following form:

$$\Delta t \leq \min\left(\frac{\Delta x_i A_i}{Q_{it}}\right) \qquad \forall i, t \tag{4}$$

The Courant condition requires that each time interval Δt of simulation must be such that the flow volume (i.e. the product of Δt and Q_{it}) in any fully mixed reach segment must be no greater than the volume of water in that segment, which implies that the flow into any segment remains in that segment in the given time period. In simulation models based on the Eulerian approach, the Courant condition limits the user to a maximum value of the time step interval for a given grid segmentation, and shorter time step intervals increase the computational time of the entire simulation.

Despite the presence of an Eulerian-style fixed computation grid in SWQ, the model avoids the Courant condition described above by incorporating key elements of the Lagrangian methodology. The Lagrangian approach consists of tracing the trajectories of contaminant particles from their destination to their origin. These trajectories are called characteristic lines. The method tracks a characteristic line backwards from the arrival or destination site to the departure or origin site (or 'foot' of the characteristic line). The

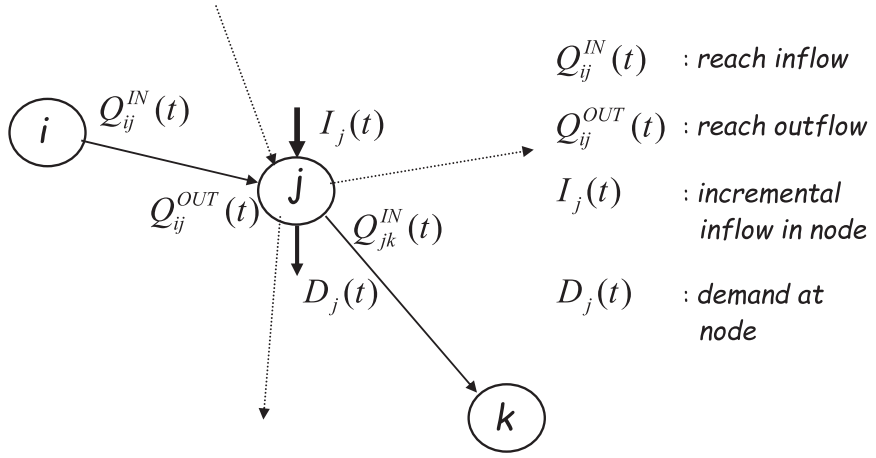

Figure 1. Node representation of a stream system network and flow variable notation.

Lagrangian method requires knowing constituent concentration values at these arbitrary particle points (the feet of characteristic lines). However, the Lagrangian approach typically deploys a continuously deforming coordinate system, meaning that there is no convenient fixed computational grid over which calculations are always performed in every time period. Rather than employing a continuously deforming coordinate system, semi-Lagrangian approaches employ a fixed grid of nodes at which concentrations are calculated. The concentration of constituents at any fixed point in the grid is determined by backtracking upstream in space to where that particle would have been in a previous time step, irrespective of how far upstream the foot of the characteristic line is. The required concentrations at the foot of a characteristic line can be interpolated from nearby nodal values. In this way, semi-Lagrangian approaches like SWQ combine the advantages of a fixed grid (Eulerian) with the Lagrangian advantage of having no limitations to simulation time step. Note that the interpolation algorithm can have an important effect on the accuracy of advection-dominated solutions. For example, travel time is very sensitive to the approach employed to conduct spatial interpolation. Different spatial interpolation algorithms can be implemented in a Lagrangian-based approach, including linear, quadratic, cubic spline, and taut spline interpolation (Ruan and McLaughlin 1999). Linear and quadratic interpolators have been the more widely used in multidimensional transport applications than higher order interpolators (Goode 1990). In a wide range of practical applications, a linear interpolation is adequate.

To demonstrate how SWQ implements the Lagrangian approach, consider a stream divided into discrete reaches, as displayed in Figure 2. To compute the concentration C of some constituent at the node *i* at the end of some period *t* of duration Δt, SWQ backtracks upstream to find all sources of the constituent whose time of travel to the node *i* is just equal to or greater than the simulation time-interval Δt. Since these sources are locations that typically do not coincide with predefined nodes, the required concentrations must be interpolated from nearby nodes. In Figure 2, the upstream sources of contaminants (feet of the characteristic lines) that will arrive at the fixed destination node *d* at the end of period *t* (or beginning of period t + 1) are located at locations M, N, O and I.

These Lagrangian coordinates (M, N, and O), one for each flow path, are computed using the time of flows in each reach along the flow paths in the period *t*, for those reaches that are less than or equal to one simulation time step upstream. (Exceptions to this process occur when the total time of flow to an initial node is less than one simulation time step). For example, suppose the concentration of some constituent at the end of period t is to be computed at node site d shown in Figure 2. Consider the flow path from node 1 to node d. Assume the time of flows, in period *t*, of the consecutive reaches upstream from node d to node 1 are 0.3, 0.5, 0.1, 0.2 and 0.2. Working upstream from node d, the point (site M)

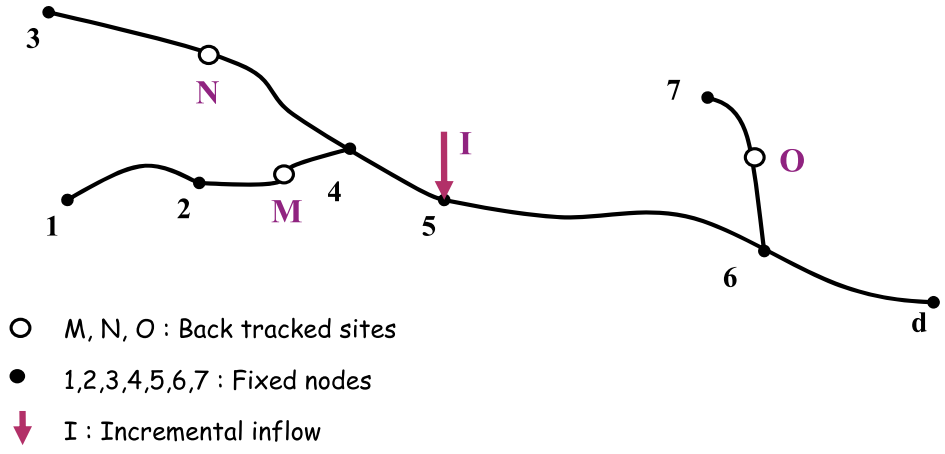

Figure 2. Backtracked locations and fixed nodes in the Lagrangian approach to predicting a constituent concentration at downstream node *d*.

at which the total time of flow to node d is exactly one simulation time step is between nodes 2 and 4. Since the time of flow from node 4 to node d and from node 2 to node 4 are respectively 0.9 and 0.2, that places site M halfway up the reach between node 4 and node 2.

The approach to computing a constituent concentration $C_d(t)$ at the end of period t at node d is to first compute the concentration ($C_M(t\text{-}1)$, $C_N(t\text{-}1)$, $C_O(t\text{-}1)$, $C_I(t\text{-}1)$) at each of these backtracked locations *M, N, O* and *I* one simulation time step earlier. To do this, backtracking is continued until reaching the next upstream node where the concentrations at the end of each previous simulation period are known. Consider site *N*, for example. The next upstream node site is node 3. The time of flow from node 3 to site *N* must be computed by taking the actual simulation period into account. For example, if in period t-1 the time of flow from node 3 to node 4 were τ_{34}, then interpolating over space, the time of flow from node 3 to site *N* is:

$$\tau_{3N} = \frac{L_{3N}}{L_{34}}\tau_{34} \tag{5}$$

where L_{3N} is the distance between node 3 and site *N*, and L_{34} is the distance between nodes 3 and 4.

If the time of flow in period t-1 between nodes 3 and *N* exceeds 1 but not 2, then a new site N′ is found that is exactly 2 simulation time steps away from node *d*, and the process to be described continues with the appropriate simulation time periods. Similarly for travel times exceeding 2. Assuming that τ_{3N} is no greater than 1, the next step toward calculating the concentration $C_N(t\text{-}1)$ at point *N* is to find $C_3(t\text{-}1\text{-}\tau_{3N})$ at node 3. This can be done by interpolating over time at node 3 between $C_3(t\text{-}2)$ and $C_3(t\text{-}1)$:

$$C_3(t-1-\tau_{3N}) = C_3(t-2)(\tau_{3N}) + C_3(t-1)(1-\tau_{3N}) \tag{6}$$

Now $C_N(t\text{-}1)$ is simply $C_3(t\text{-}1\text{-}\tau_{3N})$ transported over a period of τ_{3N} during simulation period t-1. Similarly for sites *M, O,* and *I*. The kinetic process of this constituent is then modeled using appropriate equations *f(C)* as defined in any text on water quality modeling.

Finally, consider the situation where the only known concentrations of some constituents are less than a simulation time step upstream of some node of interest. For example, suppose the time of flow, τ_{12}, from node 1 to node 2 is less than a simulation time step. In this case, since the concentration of the constituent at node 1 is assumed to be constant over the entire simulation time step, no interpolation over time is needed to compute the concentration at node 2 at the end of the simulation period *t*.

Different flows Q with different downstream (node *d*) concentrations, $f_{id}(C_i)$, coming from locations i = *M, N* and *O* and the incremental flow I are completely mixed to obtain the concentration at point *d* at the end of period *t* (or equivalently at the beginning of period $t+1$). Omitting all the *d* and *t* subscripts:

$$C = \frac{Q_M f_M(C_M) + Q_N f_N(C_N) + Q_O f_O(C_O) + Q_I f_I(C_I)}{Q_M + Q_N + Q_O + Q_I} \tag{7}$$

Point withdrawals can also be simulated by providing demand flows at the appropriate nodes in each time step. Steady-state discharges and concentrations of these inflows must be provided by the user. Initial concentrations of constituents at each node must also be supplied.

2.1.2 Contaminant fate and transport

Two important transport mechanisms define the fate and transport of a contaminant: advection and diffusion. Advection results from flow that is unidirectional, and it moves the constituent with the fluid velocity *v*. If the velocity field is uniform, the advection does not change the spatial distribution of the concentration *C* of the constituent. The flux *F* due to advection equals velocity *v* times concentration *C*:

$$F = vC \tag{8}$$

Diffusion refers to the movement of the constituent in the direction of decreasing concentration of the constituent (e.g. *x* direction). The flux F_x is proportional to the gradient of concentration (Fick's first law of diffusion):

$$F_x = -E_x\frac{dC}{dx} \tag{9}$$

where E_x is the diffusivity that must be estimated from tracer experiments or other empirical data. The minus sign indicates a net transport in the opposite direction of the concentration gradient. The one-dimensional form of the advective-dispersion equation for computing the change in average cross-sectional concentration of a constituent C, [mg/l] is:

$$\frac{\delta C}{\delta t} = \frac{\delta}{\delta x}\left(E_x\frac{\delta C}{\delta x}\right) - \frac{\delta(vC)}{\delta x} - kf(C) \tag{10}$$

where *v*: average cross-sectional velocity [m/sec];

E_x: longitudinal dispersion coefficient [m^2/sec];

The last term on the right-hand side of Equation (10) (*f(C)*) captures the kinetics of the reactions involving the constituent. The Eulerian approach integrates the transport Equation (10) over a fixed computational grid. Numerical problems (Yeh *et al.* 1992) in this approach are due to the first order advection term and can be reduced by using both fine grid size and small time step. The Lagrangian approach tracks changes in a series of computational nodes moving with the flow. Therefore, the advective term is eliminated by moving these nodes with the average longitudinal velocity. The Equation (10) becomes (Schoellhamer 1988):

$$\frac{\delta C}{\delta t} = \frac{\delta}{\delta \gamma}\left(E_\gamma\frac{\delta C}{\delta \gamma}\right) - kf(C) \tag{11}$$

where *k*: temperature-dependent constant [1/day] and γ is the new Lagrangian coordinate, such as sites *M, N, O* and *I* for each source of constituent reaching node *d* in Figure 2.

Diffusion is the predominant transport phenomenon in estuaries and can be neglected relative to advection if:

$$\frac{4kE_\gamma}{v^2} << 1 \tag{12}$$

This is usually true for rivers but is not true for estuaries where the velocity *v* is usually smaller and E_γ is usually higher than for rivers.

When dispersion is neglected compared to advection, Equation (11) becomes:

$$\frac{\delta C}{\delta \tau} = -kf(C) \tag{13}$$

2.1.3 Reaction fundamentals

The SWQ Model analyses the fate and transport of constituents using the suite of equations presented in Annex A. SWQ Model includes a simplified heat balance model for the computation of resulting temperature. Here we focus only on the details relevant to DO and BOD, because these constituents are the focus of our model comparison. Different chemical equations are used to represent the kinetics of the reaction involving these constituents. Although a first-order kinetic relationship is used herein, higher-order kinetics can be used also.

2.2. Design of model comparison exercise

Here we use two experiments to demonstrate the ways in which user-selected simulation parameters (time step duration and grid segmentation) interact with SWQ's SL algorithms to impact accuracy and potential computational time in comparison to an Eulerian model, QUAL2K. QUAL2K is a river and stream water quality model that is intended to represent a modernized version of the QUAL2E model (Brown and Barnwell 1987). Model comparisons were conducted for (1) steady state flow and steady state concentration (i.e. flow rates and concentration inputs were assumed to be constant over time at all locations), and (2) steady state flow and nonsteady state concentration (a 24-hour cycle was simulated, during which time concentration was linearly varied on an hourly basis; see Figure 3). Our focus here is on comparing model performance with respect to accuracy and stability, so we confine our analyses to two well-studied water quality constituents – Dissolved Oxygen (DO) and Biochemical Oxygen Demand (BOD).

For the steady state model comparisons, a hydraulically uniform theoretical 10 km river reach was maintained in steady state for the duration of simulation, with a point source input and an upstream (headwater) source at x = 0 km. First-order BOD decay and oxygen reaeration were the only two processes impacting DO and BOD, which remained constant throughout the system (longitudinal dispersion was not considered). Additional assumptions are summarized in Table 1. This allowed us to produce exact analytical solutions for DO and BOD concentration over time, to serve as a benchmark against which to compare the two models.

For the second (nonsteady) comparison experiment, we only vary concentration over time (not flow), to enable direct comparison of the two models – while QUAL2K does not permit a scenario in which flow varies among time periods, it does offer a feature that permits 24-hour (diel) simulations wherein concentration inputs, not flow, are permitted to vary. This feature does have limitations, which guided the model comparisons: simulations are required to be exactly 24 h in duration; and concentration inputs at the headwater source are required to be specified on an hourly basis, and to be connected by linear segments. The model configuration for this comparison (important assumptions for which are given in Table 1) was closely based on the steady state model system, although some changes were made, such as to the velocity and values of the kinetic parameters. Figure 3 summarizes the input concentrations at x = 0 km.

Simulations with both SWQ and QUAL2K were conducted for a variety of combinations of simulation time step duration and grid segmentation schemes. The systems in both models were segmented into n equally spaced computational cells, which were varied among $n = 1$, $n = 2$, $n = 5$, $n = 10$ and $n = 20$. The numerical method time step duration was also varied, although the models could not always be evaluated for identical time step durations due to a variety of time step restrictions in QUAL2K (including segmentation-dependent maximum time step restrictions). SWQ has two different time steps of interest. The model's general simulation time step, which is comparable to that of QUAL2K in meaning, is used in the backtracking step, and was kept constant at $\Delta T = 1$ h during all simulations for simplicity. This time step is the interval at which the model produces new concentration estimates at each location. However, SWQ has a second time step–the numerical method (fourth-order Runge–Kutta (RK4)) time step – that is used to transfer a concentration from a backtracked location (in our case, 1 h upstream) to a downstream location and time of interest. This SWQ-specific numerical method time step was varied across a range of durations,

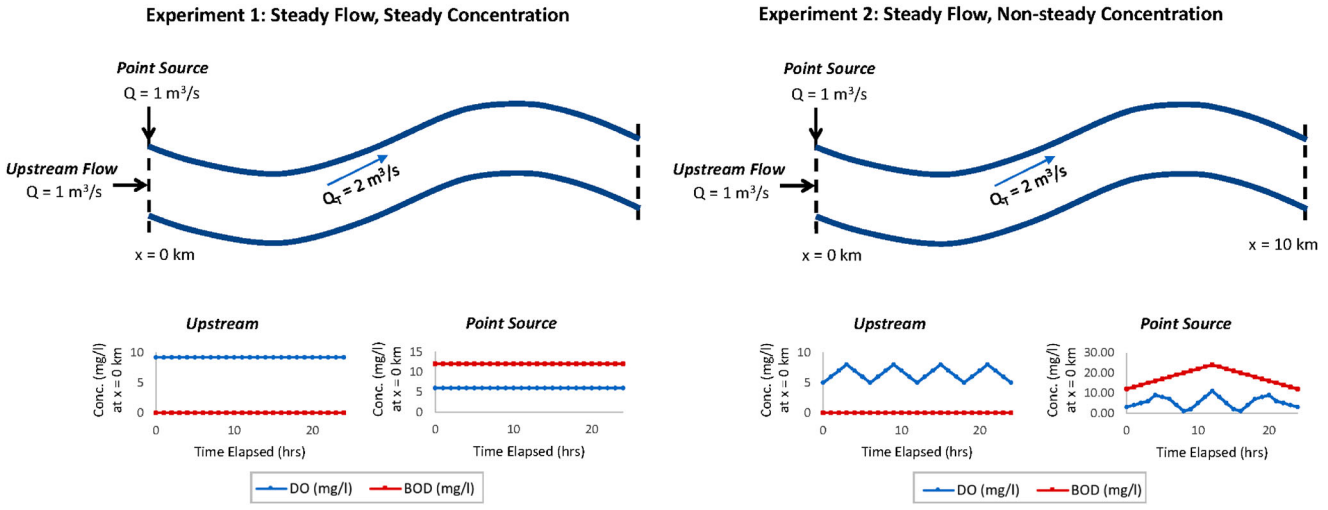

Figure 3. Schematic of the 10-km reach of river considered in this model comparison exercise, which compares the SWQ model to the QUAL2K model. Experiment 1 (top) is steady state flow and concentration, whereas Experiment 2 (bottom) is non-steady state flow and concentration. There are two sources of input to the system: upstream flow from the portion of the river upstream of the modeled reach, and a point source of waste effluent discharge. Both sources are assumed to be fully mixed at x = 0 km. Both sources provide a steady flow of 1 m^3/s in both experiments, but the DO and BOD concentrations vary over a 24-hour period according to the figures shown next to each source in each experiment.

0.164–6.547 h, to evaluate the implications for solution stability and accuracy. Alternatively, QUAL2K only has one time step a user can select, and it reflects both the general simulation time step (i.e. the interval at which new concentrations are simulated), as well as the numerical method time step. We explored a variety of time step sizes for QUAL2K, but simulations with values of time step size below 0.375 h were not included for QUAL2K because additional improvements in accuracy were not obtained for such time steps.

2.3. Model evaluation results

2.3.1 Comparison of SWQ and QUAL2K performance for steady state flow and concentration

First we explore the impact of the following factors on model performance: extent of stream segmentation, numerical method time step size, and numerical method (i.e. Euler versus Runge–Kutta) used for integration and simulation duration. Figure 4 explores the impact of segmentation and time step size on model performance for a system with steady state flow and concentration. We don't show all variations of time step size and segmentation in Figure 4; rather we show examples of experimental outputs that highlight key insights. Figure 4 shows the QUAL2K and SWQ spatial approximations of DO and BOD concentrations for $n = 5$ and $n = 10$ computational cells, respectively. (Results for $n = 1$, $n = 2$, and $n = 20$ are provided in the Supporting Information in Figure S1, S2, and S5). Recall, however, that n is not the only means by which users of the two models can control accuracy. Accordingly, Figure 4 presents multiple QUAL2K-model evaluations to demonstrate the impact of simulation time step size and numerical method on accuracy. On the same figures, multiple sets of data points are also plotted for SWQ, where each set of points represents a particular spatial evolution of concentration corresponding to a particular time step value. QUAL2K data are plotted for two time steps and two numerical methods, whereas spatial results for six different numerical method time step values (up to 1.31 h) are shown for SWQ. While there is no accuracy-based restriction to the SWQ numerical method time step, the numerical method in QUAL2K is restricted to a maximum value, and this is why not all evaluations of both models could be conducted using the same time step values. If no data are plotted for a particular value of time step size in QUAL2K, or for a particular numerical method (i.e. Euler or RK4 in QUAL2K), this indicates that no significant additional improvement (greater than 1% or 2%) in accuracy was obtained for such a model configuration in comparison to the base cases for those configurations (i.e. compared to higher time step size or compared to the lower accuracy Euler method). For example, if a set of points is plotted for a simulation in which integration was performed with an Euler method but not for a RK4 method, this indicates that the RK4-based simulation did not produce significantly different results than the Euler-based simulation. Finally, note that all figures contain the analytical solutions to the DO and BOD equations to elucidate the accuracy of predictions.

Before interpreting results, first note some important differences between the models. QUAL2K segments are completely mixed, which naturally creates concentration discontinuities at the interfaces of elements. Conversely, SWQ produces concentration estimates at specified locations, rather than for each cell. At the end of each computational element into which the stream is segmented, anywhere from five to seven data points are plotted for each constituent to represent SWQ output, where each data point represents an SWQ concentration prediction for a given location and a given Runge–Kutta time step selection with which the simulation was conducted.

Figure 4 shows that increasing the number of computational elements resulted in clear improvements in the accuracy of concentration predictions in QUAL2K. For values of segmentation beginning at $n = 1$ and proceeding through $n = 10$, SWQ appears to be far more likely to provide a concentration prediction within reasonable proximity to the analytical value at each location if a random time step were to be chosen. In general, especially as n increased, improvements in the numerical method time step size resulted in improvements to accuracy in both models. Increased segmentation

Table 1. Input data and assumptions for (1) steady flow and concentration and (2) steady flow and nonsteady concentration comparisons of SWQ and QUAL2K.

	Steady State Flow/ Concentration		Nonsteady State Concentration	
	Headwater	Point Source	Headwater	Point Source
Flow rate [m^3/s]	1	1	1	1
Velocity [m/s]	0.3	–	0.3	–
DO conc. [mg/l]	9.2	6	See Figure 3	See Figure 3
BOD conc. [mg/l]	0	12	See Figure 3	See Figure 3
Temperature [°C]	20		20	
BOD decay rate [1/day]	40		5	
DO reaeration rate [1/day]	10		7.5	
DO saturation conc. [mg/l]	9.2		9.2	
Elev. [m above sea level]	0		0	
Length of system [km]	10		10	
T_s, travel time [hr]	6.55		1.637	
Combined flow rate [m^3/s]	2		2	
Combined velocity [m/s]	0.42		0.42	
Dispersion [m^2/s]	0		0	
QUAL2K numerical method time step [hr]	$\Delta t = 0.375, 0.75, 1.5, 3.0$		$\Delta t = 0.375, 0.75, 1.5, 3.0$	
SWQ model time step [hr]	$\Delta T = 1$		$\Delta T = 1$	
Number of computational elements, n	$n = 1, 2, 5, 10, 20$		$n = 1, 2, 5, 10, 20$	
SWQ numerical method time step [hr]	$\Delta t = 0.164$-6.547		$\Delta t = 0.164$-6.547	
Numerical Integration	SWQ: 4th Order Runge-Kutta QUAL2K: Euler, 4th Order Runge-Kutta		SWQ: 4th Order Runge-Kutta QUAL2K: Euler, 4th Order Runge-Kutta	

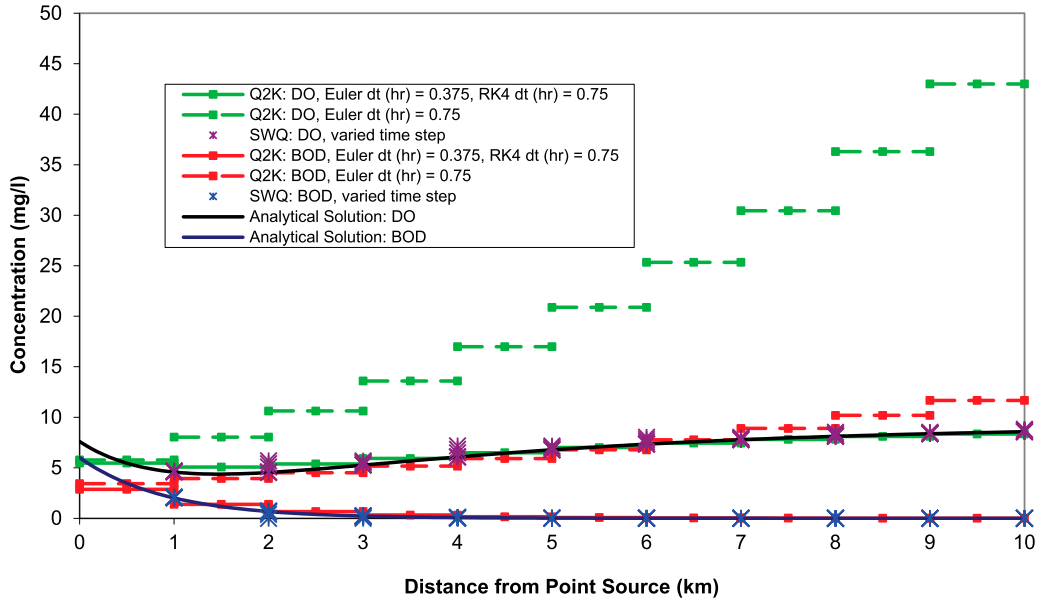

Figure 4. Experiment 1 (steady state flow and concentration) SWQ and QUAL2K (Q2K) simulation results, and analytical solution for DO and BOD concentrations for the entire profile of the modeled 10-km long reach of river (see Figure 3). Results correspond to a system with velocity = 0.42 m/s and n = 5 segments (top figure) versus n = 10 segments (bottom figure). Time step size (dt) was varied in both models, and numerical method was varied in QUAL2K. Note that Q2K concentrations in one case (using the Euler numerical method) exceed the oxygen saturation concentration as a result of accuracy loss from the Eulerian approach, owing to the combination of time step and grid segmentation.

did not impact accuracy nearly as significantly in steady state SWQ simulations as it did in QUAL2K, whereas reduction in the numerical method time step size often provided significant accuracy improvements.

Figures S3.18–S3.22 display, for $n = 1$, $n = 2$, $n = 5$, $n = 10$ and $n = 20$, respectively, the square root of the ratio of the sum of squared errors (SSE) from SWQ to the SSE for QUAL2K for DO, as a means of capturing how well the two models replicate the entire spatiotemporal profile of concentration. The SSE is used to capture the difference between modeled and analytical concentrations. The SSE for QUAL2K improved with increased segmentation and decreased time step, whereas SSE for SWQ was primarily improved by decreasing the numerical method time step. SWQ was not expected to result in drastically improved estimates of concentration with increasing n because segments are not assumed to be completely mixed in SWQ and thus numerical dispersion error is not reduced in SWQ as it is in QUAL2K by increasing the extent of segmentation.

Since SWQ performs temporal interpolation, interpolation-based loss in accuracy is more likely for simulations in which flow and concentration vary over time at each location. As there is no necessity for segmentation, SWQ offers a significant computational advantage when concentrations are desired at relatively few points in the system.

Additionally, improvements in QUAL2K accuracy obtained by increasing n proceeded at a much slower rate at the location of the low point on the DO sag curve (as seen in Figure 4). This is a typical problem associated with the Eulerian approach, because the completely mixed sections (and numerical dispersion) tend to flatten and spread at sharp concentration fronts. Conversely, SWQ appeared to maintain consistent accuracy characteristics regardless of the segmentation specified, including reasonable representations of the DO low point. In general, for the same time step and segmentation, SWQ provided better accuracy. As a solution to this problem in QUAL2K, one could increase the segmentation surrounding the location at which the low point is expected to occur, thereby producing a more accurate estimation of the low point value. However, a modeler may not be able to prepare a confident estimate of this location prior to simulation. Even if one were able to develop a more confident estimate of this location by first conducting a trial simulation, a series of small segments in QUAL2K at any point in the system would create a time step limitation for every segment in the system, because the model time step applies to all segments.

Selection of a time step in QUAL2K that violated the courant condition occasionally produced a drastic reduction in accuracy. The reach travel time is approximately 6.5 h, so time steps should be limited to a maximum value of about 6.5/5 = 1.3 h to avoid violating the courant condition, which is less than the 1.5-hour time step size we explored. QUAL2K was developed within an implicit framework that technically offers stability in such circumstances, but implicit frameworks do not prevent accuracy losses. While QUAL2K did appear to prevent the simulation from proceeding when extreme violations occurred, this unfortunately made it difficult to compare both models with increasingly larger time steps, because QUAL2K will not permit serious courant condition violations. Regardless, from a modeling standpoint, such sensitivity to user-specified parameters is undesirable. For example, knowing that increasing the value of n should improve accuracy in QUAL2K, a modeler might increase $n = 2$ to $n = 5$ and maintain the same time step duration. For a time-step duration of 1.5 h, this increase from $n = 2$ to $n = 5$ would have resulted in decreased accuracy due to the discrepancy between the time step size and grid cell travel time.

While the computational advantage offered by SWQ may appear to be rather modest for the small system and travel time considered previously, the advantages become more obvious for larger systems with increased advection and high rates of change associated with the kinetic processes.

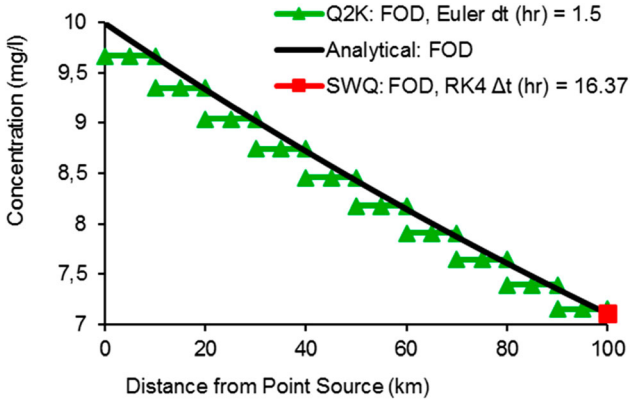

Figure 5. SWQ and QUAL2K (Q2K) simulation results, as well as analytical solution, for the concentration of a constituent subject to first-order decay (FOD).

In Eulerian models, these circumstances require increased segmentation and smaller time steps. Consider a reach that is 100 km in length, with a velocity of 1.7 m/s. Assume the goal of simulation is to determine the concentration of a constituent subject only to first-order decay (with a decay constant of 0.5 day^{-1}) to within 0.05 mg/l at location x = 100 km. In QUAL2K, about $n = 10$ reaches were required to obtain the arbitrarily specified accuracy, with a maximum time step of 1.5 h. In SWQ, the requisite accuracy was obtained using one element and a time step of 16.34 h. Figure 5 shows results from both models. The user is relieved of any requirement to navigate tradeoffs between time step and segmentation with SWQ, and SWQ produced identical accuracy to QUAL2K with a time step ten times larger, and with ten times fewer segments.

2.3.2 Comparison of SWQ and QUAL2K performance for steady state flow and non-steady state concentration

Outcomes of this experiment share some similarities with the steady state concentration experiment. For example, increased segmentation and decreased time step values once again improved accuracy (in terms of the closeness of concentration predictions to the analytical solution) at each of n locations in QUAL2K. We leave many of the figures demonstrating these outcomes to the *Supporting Information* document, because we have already discussed these outcomes at length for the steady state concentration case in the previous section.

Figure 6 (which plots DO concentration for $n = 10$ at x = 10 km) highlights several of the most important model output characteristics that emerged during model comparisons that are unique to the non-steady state concentration nature of the experiment. Significant deterioration of accuracy was observed in QUAL2K when Euler numerical method time step durations violated the Courant condition (i.e. exceeded the cell travel time). See the time series in Figure 6 corresponding to an Euler time step of 0.1875 hours, for example. The extent of accuracy loss depended on the magnitude of the time step relative to the rates of change associated with the governing kinetic parameters. From a practical modeling standpoint, a sensitive model with the potential for inaccuracy is undesirable. If the modeling application happened to involve fluctuating concentrations, then numerically-based fluctuation of concentration could be indiscernible from physically-based fluctuation. The best solution possible in QUAL2K for a given value of n often demonstrated a variety of numerical deficiencies, including numerical dispersion, phase error, valley elevating, and peak elevating, some of which are shown in Figure 6. The simulated 24-hour concentration profile should be comprised of linear segments containing several sharp peaks and valleys. Curvature should only appear in the spatial profile. Significant increases in segmentation in QUAL2K were required to reduce these effects.

In SWQ, high accuracy results were obtained for a variety of combinations of time step duration and segmentation selections. SWQ returned results with better accuracy than QUAL2K for identical segmentation and time step selections. In SWQ, the extent of segmentation did not significantly influence overall accuracy, while time step size did. SWQ was shown to demonstrate two primary forms of loss in accuracy: (1) inaccuracy resulting from the size of the numerical method time step applied in the forward-tracking

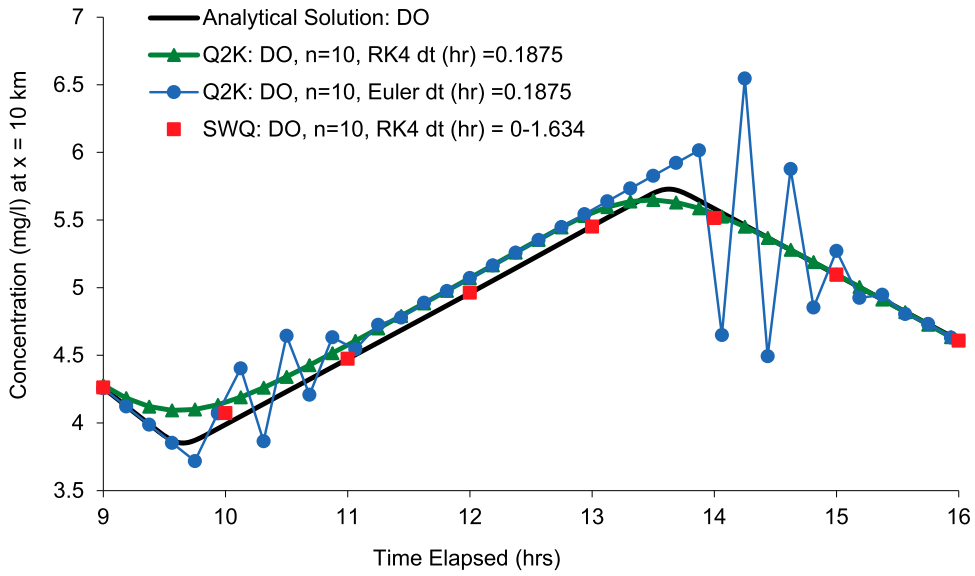

Figure 6. Temporal (24-hour) DO concentration profile for SWQ and QUAL2K (Q2K) at x = 10 km for n = 10 computational elements. An approximate analytical solution is also provided. Numerical method time step duration was varied in both models, and numerical method was varied in Q2K.

step, and (2) error resulting from loss of information about peaks and valleys (peak and valley clipping) that can occur during the interpolation step. Regarding the latter issue, SWQ linearly interpolates between concentrations at different times at each location to which the algorithm backtracks. The result is that a large SWQ model time step duration (not the numerical method time step) can be large enough to cause a linear interpolation that coarsely transects regions of rapid concentration change (e.g. peaks and valleys), which appears as peak and valley clipping in Figure 6. Fortunately, this is not a precursor to numerical dispersion in SWQ, because conservation of mass is not rigidly enforced. One important difference between the models that impacts the interpretation of these results is that concentration values produced by SWQ are reported only on an hourly basis, whereas the time increment at which QUAL2K reports concentration values is equal to the value of the numerical method time step. In order to obtain SWQ output on a sub-hourly basis, and to more effectively capture the minima and maxima, the duration of the SWQ model time step would need to be reduced.

3. Application on Sava River, Slovenia

The previous section provided a quantitative comparison of SWQ and QUAL2K with respect to issues such as grid segmentation, time step, and accuracy using a didactic 10 km long river reach. In this section, we focus on demonstrating that SWQ can produce high-fidelity simulations of key constituents in a real river system, and that SWQ does so with comparable accuracy to QUAL2K when both models are optimally configured. To perform the comparison, we used QUAL2E, rather than QUAL2K. QUAL2E is the predecessor to QUAL2K, but QUAL2E has a longer history of application in the Sava River Basin (Drolc and Končan 1996, 1999). For the purposes of this study, QUAL2K and QUAL2E have essentially the same functionality, including one-dimensional mixing (i.e. flow is well-mixed vertically and laterally), steady state hydraulics (i.e. steady flow), diurnal water quality kinetics and heat budgets, and point and non-point constituent loading and abstraction.

3.1. Sava River background

The Sava River was Yugoslavia's major river prior to the dissolution of the Socialist Federal Republic of Yugoslavia in the early 1990s. Since then, it has become an international river of 4 former Yugoslav republics (Bosnia–Herzegovina, Serbia, Croatia and Slovenia). The Sava River is a tributary of the Danube River and contributes almost 25% of the Danube's total discharge. From the confluence of its longer headwater the Sava River is 990 km long. The modeled section is located in the Upper Sava downstream of the confluence of Ljubljanica River, where Sava River has an average longitudinal slope close to 10%, and is torrential in character. The hydrologic balance is heterogeneous in temporal distribution, with long-term flow average ranging between 28.9 m^3/s in summer and 175 m^3/s in winter (Ogrinc *et al.* 2008). Discharge of organic degradable wastewater is the key factor that affects the dissolved oxygen (DO) concentration in this part of Sava River, as Ljubljanica River receives significant volumes of industrial and municipal wastewaters directly from sewage stations. Biological elements such as oxygen regime parameters (DO, BOD_5, COD, $KMnO_4$, TOC) are considered obligatory parameters to measure and control in order to maintain compliance with Directive 2000/60/EC of the European Parliament (EU WFD). Under extreme conditions, DO might even drop to zero, as in 1983 when the occurrence of low flow of 14 m^3/s and high-water temperatures (of 22°C) created widespread and persistent anoxic conditions.

The Sava River Basin is one of South-Eastern Europe's major drainage basins, covering a total area of approximately 97.713 km^2, and hosting a population of roughly 8.5 million. The International Sava River Basin Commission is an international organization established for the purpose of implementing the Framework Agreement on the Sava River Basin (FASRB). FASRB has the objective of establishing an international regime of navigation on the Sava River and a sustainable water management plan, as well as undertaking measures to prevent or limit hazards. Specifically, a sustainable integrated water resource management 'would provide water in a sufficient quantity and of appropriate quality for all kinds of use/utilization' (http://www.savacommission.org/mission). A key activity has been the preparation of the first Sava River Basin Management Plan (SRBMP) in accordance with the EU WFD. In 2016, an important step in this regard was the development of the 2nd Sava River Basin Analysis Report (http://www.savacommission.org/publication). The greatest population density occurs near Ljubljana, while the upper part of the basin is covered mainly by forests (>50%) with subalpine vegetation occupying ~35%. Point sources of organic pollution from treated domestic sewage are the greatest source of organic materials discharged to the river and have been considered critical sources of pollution that exert significant pressure on the river (Table 2).

Many urban areas in the basin have no, or have insufficient, wastewater treatment and are therefore key contributors of organic pollution. Under the Water Framework Directive, there are a number of EU directives that came into force as legislative acts in Slovenia. The application of the Urban Waste Water Treatment Directive in the SRBMP aims to phase out all discharges of untreated wastewaters by 2023 through the construction of wastewater collection and treatment systems. These measures should result in a considerable reduction (26.4%) of BOD.

3.2. SWQ and QUAL2E application to Sava River

Initially, we performed a series of sensitivity runs to identify key parameters in the models. Based on these analyses, we identified the following parameters as the most relevant model parameters and output variables for SWQ and QUAL2E predictions:

- Biochemical oxygen demand of the discharged wastewater (BOD) [mg/L]
- Degradation rate constant for BOD (k_d) [1/day];

Table 2. Pollution from urban areas with > 2000 Population Equivalent (PE).

		Generated Load		Emissions	
	PE	BOD (t/y)	COD (t/y)	BOD (t/y)	COD (t/y)
Slovenia	964966	21133	38743	10717	21531

- Reaeration rate constant (k_a) [1/day];
- Sediment oxygen demand rate (SOD) [mg-O/m^2/day];
- Temperature of river water (T) [°C];
- Flow rate (Q) [m^3/sec].

Drolc and Končan (1996, 1999) applied the QUAL2E model to estimate the impact of discharged wastewaters on DO in the Sava River. They considered:

1. Conditions that most critically affect DO: summer low flow, high water temperature, nighttime period;
2. Processes that affect DO in these critical conditions:
   - Biodegradation of organic wastes, BOD [mg/L];
   - Oxidation of organic matter in bottom sediments, SOD [g/m^2/period];
   - Atmospheric reaeration

In this application, SWQ divides the Sava River into three reaches, and downstream nodes are located at the point of discharge for a wastewater treatment plant, as well as at three locations where DO field measurements were made (Figure 7). SWQ considers one time interval whose duration is equal to 2 h. Because of the previous work by Drolc and Končan (1996, 1999), we use QUAL2E here, rather than Qual2K (which we compared to SWQ in section 2 of this paper). However, QUAL2E and QUAL2K have essentially the same characteristics as it pertains to this study.

Following model data, either for QUAL2E and SWQ (Table 3), were obtained in different ways:

- BOD varied according to time of day. From field data, daily range is: min 190 mg/L – max 410 mg/L;
- k_d was determined in laboratory modeling of Sava river;
- SOD was measured in situ;
- Temperature and flow of Sava River were those at the times of DO field measurements for calibration and validation;
- empirical hydraulic parameters were determined for a steady state regime on the basis of field measurements of flow, velocity, and depth.
- k_a was calculated using the energy dissipation model (Tsivoglou and Neal 1976):

$$k_a = B\frac{\Delta h}{\tau_f} \tag{14}$$

where: Δh [m] is the surface elevation change;
τ_f [day] is the time of flow in the reach;
B is a parameter [1/m].

Parameter values of SWQ could be calibrated using PEST (Doherty 2010), a model-independent software package for parameter estimation and uncertainty analysis of hydrological and environmental computer models.

SWQ assumes that the geometric and hydraulic properties in each reach are constant and calculates time of flow in each reach using equations similar to Equation (3). To compute the DO concentration in those three locations, SWQ backtracked upstream to locate all DO sources whose time of flow is just equal or greater than the user-defined simulation time step of 2 h.

Figure 8 shows the time of flow in each reach. Assuming these times of flows do not change from one time step to another, one can easily see what sites must be used in this backtracking procedure. For example, to calculate the concentrations of water quality constituents at 2 km using a simulation time step of 2 h, the most upstream sites (Sava River Upstream and Ljubljana WTP) must be used. If the quality at 7 km site is desired, the backtracking must use the 2 km site concentration values.

The performance of the proposed approach is measured by how well the identified DO concentration matched the

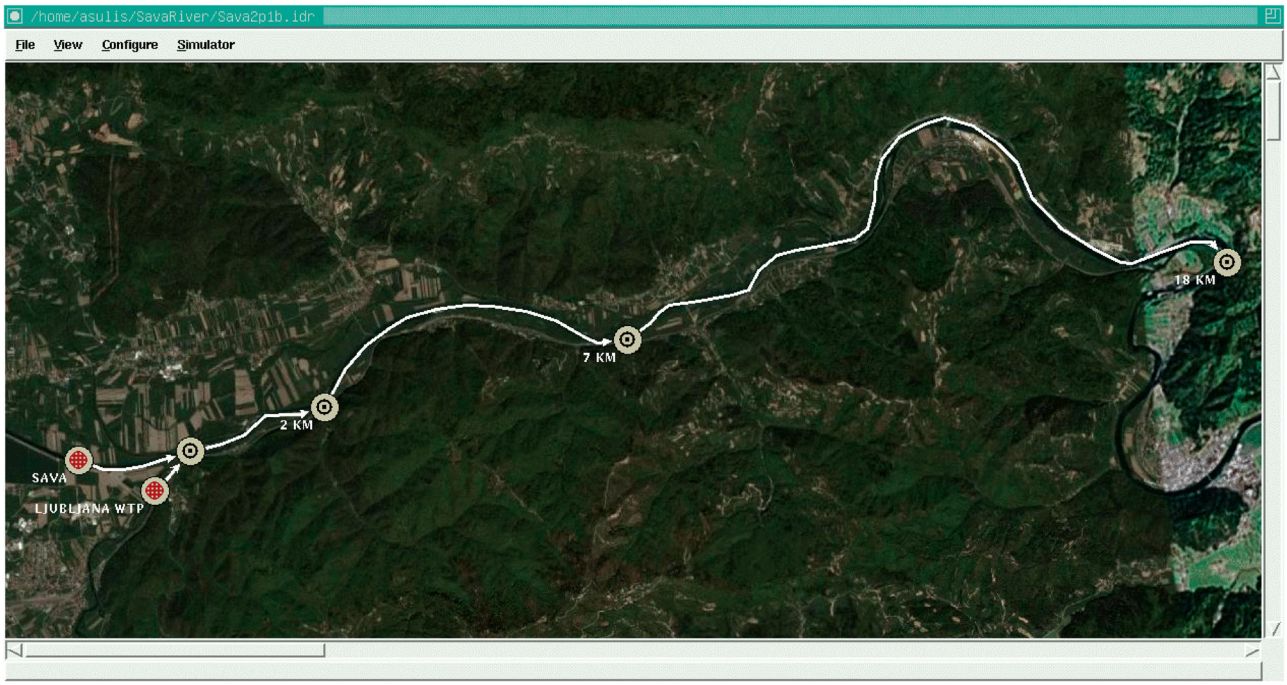

Figure 7. Study site and model domain in SWQ graphical interface.

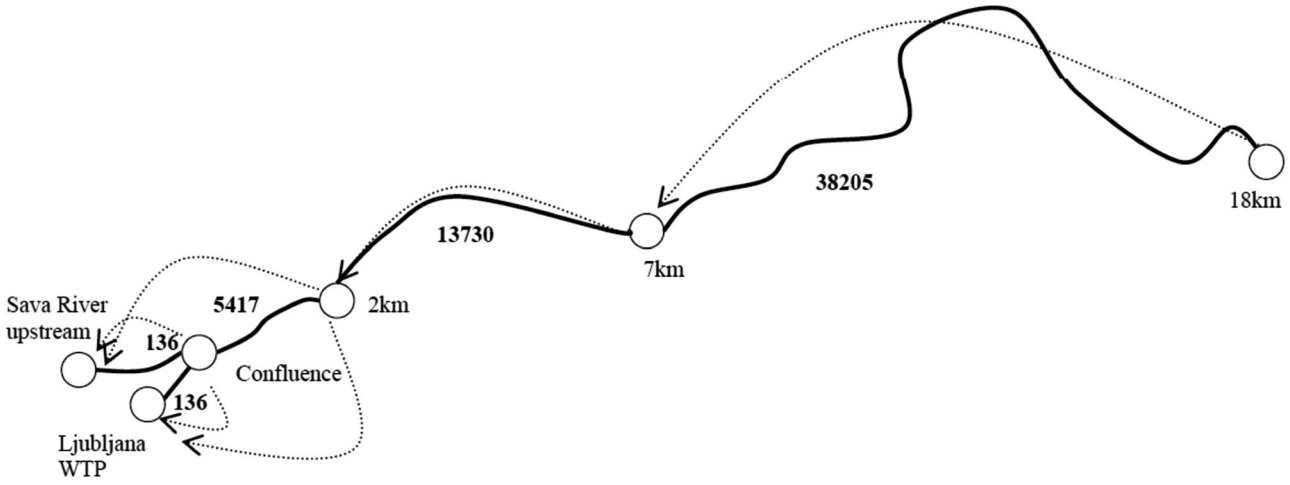

Figure 8. Backtracking approach in Sava River application (dotted lines are referred to a 2 h time period and time flows are in seconds).

true DO concentration. Validation analysis was based on field measurements at three locations in the Sava River (Figure 7): at 2Km, 7Km, and 18Km after the confluence of the Sava and Ljubljanica Rivers. The observed dissolved oxygen concentrations at these locations are shown in Table 4. These DO values are the cross-sectional averages observed early in the morning during the low flow period (Drolc and Končan 1996, 1999). Both air and water temperatures were assumed to be the same at 20°C.

Figure 9 illustrates the results of the validation analysis. Comparison of the observed DO data with model predictions suggests that both models make reasonably good predictions of DO, with the mean relative errors $\bar{\Delta}$ equal to – 4% in QUAL2E and 4% in SWQ. Specifically, SWQ tends to slightly underestimate DO in all three locations ($\Delta_{SWQ,2Km} = 5\%$, $\Delta_{SWQ,7Km} = 4\%$, $\Delta_{SWQ,20Km} = 3\%$), while QUAL2E tends to match DO in the first and third location ($\Delta_{QUAL2E,2Km} = 1\%$, %, $\Delta_{QUAL2E,20Km} = -3\%$) but significantly underestimates the critical DO ($\Delta_{QUAL2E,7Km} = -11\%$).

As the reaeration rate k_a is a sensitive parameter in SWQ, we refined the energy dissipation model (14). Many equations for k_a have been proposed in the literature and some of these are widely applied in water quality studies (see Bowie *et al.* 1985 and Orlob 1982, for comprehensive reviews). However, recent studies have demonstrated that they generally result in a poor fit with field data different from those for which each equation was originally developed (Melching and Flores 1999). Thus, none of the available equations appears to be applicable to all rivers, and values given by these equations have to be confirmed by calibration. This additional step was carried out using a least-squares approach (Little and Williams 1992), with k_a as the calibration parameter. Thus, the appropriate k_a is the value that satisfies the following:

$$MIN \sum_{i=1}^{N} (OBS_i - PRED_i)^2 \quad i \in \{2Km,\ 7Km,\ 18Km\} \tag{15}$$

where:

OBS_i is the observed value of DO at location i [mg/L];

$PRED_i$ is the DO value at location i predicted by SWQ Model [mg/L].

Compared to the energy dissipation model (14), the least-squares approach gave a small difference of +7% ($k_a = 7.38$).

The water temperature directly affects all processes in SWQ relevant to DO concentration (BOD degradation process, oxidation of organic matter in sediment, atmospheric reaeration), as well as the saturation concentration of dissolved oxygen. Data from Šentjakob monitoring station were considered in this study to perform a sensitivity analysis of DO predictions with respect to changes in stream water temperature and flow (http://www.arso.gov.si/en/). Based on flow and water quality data, previous research experience highlights this station as the most representative in downstream conditions. The reaction rate constants increase with the temperature according to the correction factor listed in Table 5.

Based on the Sava River Basin Management Plan (SRBMP), four scenarios of average seasonal water temperature (T) and river flow (Q) at Šentjakob station (Sava River upstream node in Figures 7 or 8; data in Table 6) were considered:

1. S1: historic extreme conditions in high temperature and low flow: T = 22°C and Q = 14 m^3/sec;
2. S2: summer scenario of medium flow (Q = 28.9 m^3/sec) in extreme high temperature (T = 22°C);
3. S3: summer scenario of medium flow (Q = 28.9 m^3/sec) in warm temperature (T = 10°C);

Table 3. Calibrated dataset for SWQ and QUAL2E.

Parameter	Value
Wastewater BOD [mg/L]	410
Wastewater flow [cm/sec]	1.4
k1 [1/day]	1.5
k2 [1/day]	7.38
SOD [g/m^2/day]	15
T(*) [°C]	20
Sava river flow(*) [cm/sec]	30.2

Table 4. Observed dissolved oxygen concentrations in the Sava River.

Location	Observed DO [mg/L]
2 km point	5.3
7 km point	3
18 km point	3.6

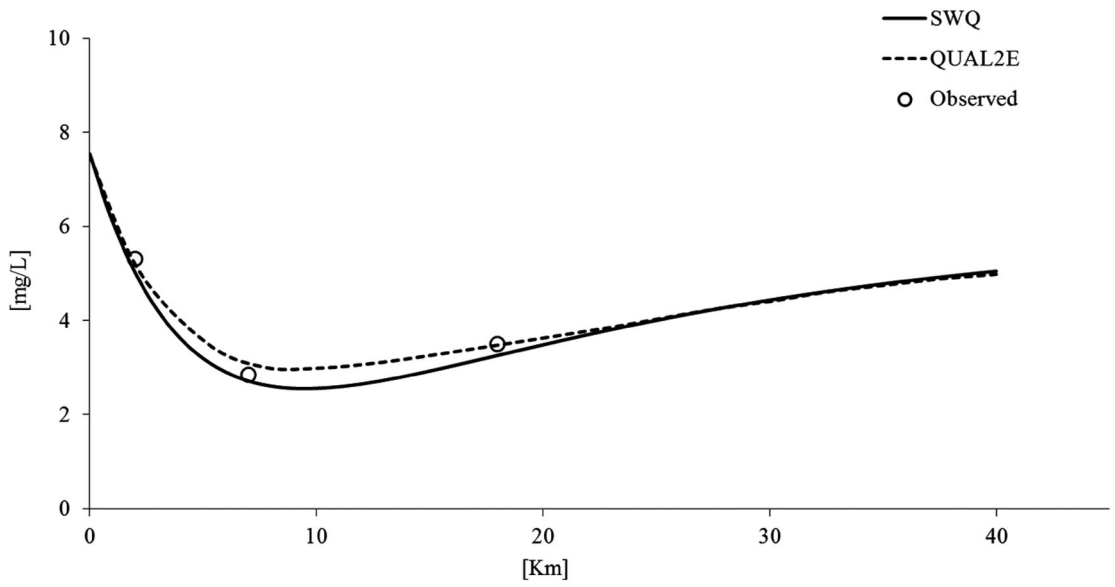

Figure 9. Validation of SWQ and QUAL2E for DO data.

4. S4: summer scenario of high flow (Q = 48.7 m^3/sec) in extreme high temperature (T = 22°C).

Concise representation of how the DO is influenced by water temperature and flow at each point along Sava River is shown in Figure 10. At each distance on the x-axis, the curves represent the sensitivity of DO in a temperature range of 10–22°C. These curves show that DO is particularly sensitive to the value of water temperature. A 50% decrease in the temperature from 20°C increases the critical DO concentration by about 120%. An increase of 25% in temperature leads to a relative decrease of about 55% in the critical DO. Increasing the flow in Sava river impacts on DO due to the dilution of waste discharges with higher quality water, the increase in the k_a values and the decreased time of flow to any given location, and hence the less time for BOD decomposition. All these factors shift the minimum DO concentration point downstream as the flow increases (Orlob 1982).

Table 5. Temperature correction coefficients.

Rate Coefficient	Value of Temperature Coefficient (Θ)
BOD	1.047
SOD	1.060
Reaeration	1.024

Figure 10 shows that flow augmentation has a beneficial impact on DO at all three location points, and critical DO concentration moves slightly downstream. As expected, the most critical condition with a large anaerobic area of 27 km (25 km in QUAL2E) is predicted by SWQ (Equation (14)) only when under scenario 1. It seems that large anaerobic conditions in Sava River requires both critical conditions in terms of temperature (T = 22°C) and flow (Q = 14 m^3/sec). This is consistent with the results of river water quality monitoring carried out under the SRBMP in accordance with the EU WFD. SRBMP states that Sava River possesses 'good

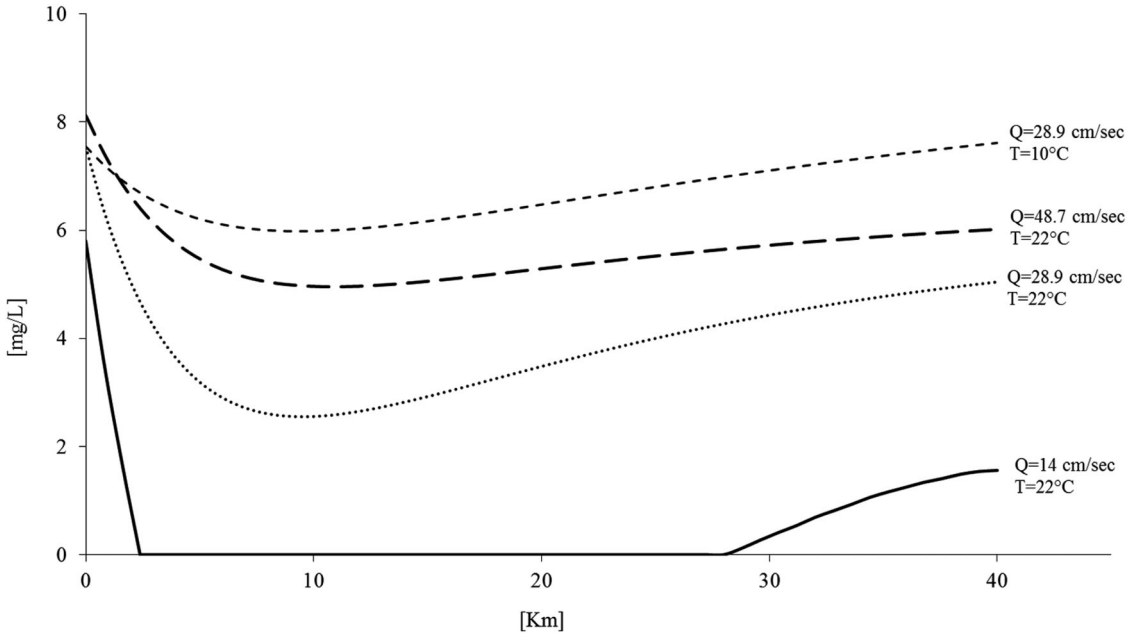

Figure 10. Comparison of Dissolved Oxygen in SWQ for different water temperature in equilibrium with atmospheric conditions and river flows.

Table 6. Upstream monitoring station.

Sampling location	Latitude N	Longitude E	Height above sea level (m)	Forest (%)	Agriculture (%)	Urban and industry (%)	Other (%)
Šentjakob	46° 06′	14° 47′	245	3.8	1.4	0.2	0.038

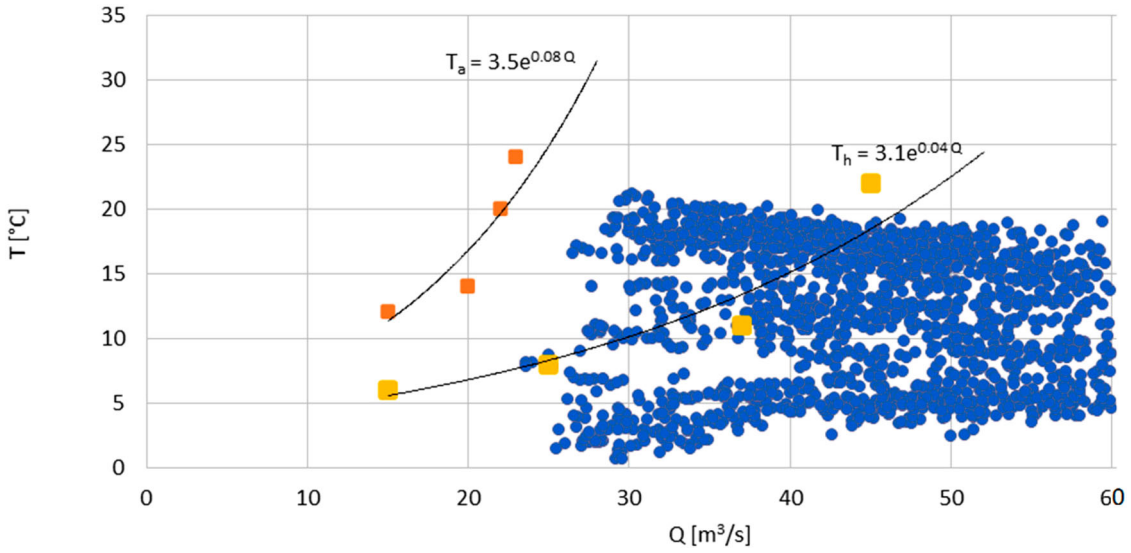

Figure 11. River flow ($Q \leq 60$ m^3/s) and temperature coupled daily measures at Šentjakob station from 10-year time series (2010-2019) (blue dots) and SWQ simulated anoxic and hypoxic conditions.

oxygen conditions' and seasonal fluctuations in DO range from 6 to 18 mg/L. Specifically, a monitoring study performed in late summer 2006 indicates that reductive conditions were present only at low flows and high temperatures (Ogrinc *et al.* 2008).

Iterative simulations with SWQ were performed to identify some threshold combinations of Q and T, $(Q, T)_{c,a}$ and $(Q, T)_{c,h}$, at Šentjakob station that produce respectively anoxic and hypoxic conditions in the simulated downstream 18 km of Sava River. Specifically, hypoxic conditions are defined as a DO concentration below a threshold value under which a water body is considered to be impaired. Anoxic conditions are more severe, and typically are defined as concentrations of 0.5 mg/L or less. Both thresholds vary for different water bodies, agencies and intended uses. Here a threshold of 5 mg/L was adopted for hypoxic conditions.

Simulation results of threshold combinations $(Q, T)_{c,a}$ and $(Q, T)_{c,h}$ are presented in Figure 11 in orange and yellow dots. Two threshold equations in the form of $T = T(Q)$ were produced with a minimum least square method from these dots:

$$T_a = 3.5e^{0.08Q} \tag{16}$$

$$T_h = 3.1e^{0.04Q} \tag{17}$$

10-year time series (2010–2019) of (Q, T) data at the Šentjakob monitoring station are shown in blue dots of Figure 11. For Q and T, seasonal variation is relatively uniform during the time with a coefficient of variation equal to 0.96 and 0.42, respectively.

Comparing the 10-year time series of Q and T in Šentjakob with the threshold Equations (16) and (17) from SWQ, we obtained that no conditions of Q and T potentially causing downstream anoxic conditions occurred at Šentjakob in the time period 2010–2019 (i.e. all blue dots are beyond the T_a equation), while a high frequency of hypoxia of 34% could have occurred (approximately 1/3 of the blue dots are beyond the T_h equation). Šentjakob station is influenced by the large city of Ljubljana with a contribution of 63.5% of the total P emission. Results highlight the necessity of improving processes of P removal at urban wastewater treatment plants to reduce the risk of downstream anoxic conditions for low flow and high temperature.

4. Conclusions

As the scale and complexity of water quality modeling studies continue to increase, the potentially significant improvements in computational time and accuracy offered by semi-Lagrangian models may become more appealing. Semi-Lagrangian (S-L) water quality models continue to occupy a relatively small presence in the literature, and the Stream Water Quality (SWQ) model was developed to help those who might find this approach appropriate for their modeling of rivers of interest and concern to them. Results of comparisons of SWQ with QUAL2K in steady and non-steady scenarios demonstrated that while both models are fully capable of producing accurate results when optimally configured, SWQ offers accuracy and stability without sensitivity to the interaction of time step size and computational grid segmentation in each particular modeling scenario. The SWQ model can certainly be improved, including the addition of higher-order interpolation techniques and calibration routines, but seems ready for use by those wishing to explore the attributes associated with the semi-Lagrangian methodology applied to water quality prediction and management.

Disclosure statement

No potential conflict of interest was reported by the author(s).

Funding

Thomas Wild's contributions to this study were supported by the U.S. National Science Foundation under grant number 1855982.

References

Alcamo, J., 2019. Water quality and its interlinkages with the Sustainable Development Goals. *Current Opinion in Environmental Sustainability*, 36, 126–140. doi:10.1016/j.cosust.2018.11.005

Ambrose, R.B., and Wool, T., 2009. Wasp7 stream transport – model theory and user's guide: supplement to water quality analysis simulation program (WASP) user documentation. U.S. Environmental Protection Agency, Washington, DC, EPA/600/R-09/100 (NTIS PB2010-104716).

Bowie, G.L., *et al*., 1985. Rates, constants, and kinetics formulations in surface water quality modeling. U.S. Environmental Protection Agency, Athens, GA, ERL, EPA/600/3-85/040.

Brown, L.C., and Barnwell, T.O., 1987. *The enhanced stream water quality models QUAL2E and QUAL2E-UNCAS: documentation and user manual report EPA/600/3-87/007*. Athens, GA, USA: U.S. EPA.

Casulli, V., and Cheng, R.T., 1990. Stability analysis of Eulerian-Lagrangian methods for the one-dimensional shallow-water equations. *Applied Mathematical Modelling*, 14 (3), 122–131. doi:10.1016/0307-904X(90)90045-7

Chapra, S.C., 1997. *Surface water quality modeling*. Long Grove, ILL: Waveland Press.

Chapra, S. C., Pelletier, G. J., and Tao, H., 2008. QUAL2K: a modeling framework for simulating river and stream water quality, version 2.11: Documentation and users manual. Civ and Environ Eng. Dep., Tufts Univ., Medford, MA.

Cheng, R. T., Casulli, V., and Milford, S.N., 1984. Eulerian-Lagrangian solution of the convection-dispersion equation in natural coordinates. *Water Resources Research*, 20 (7), 944–952. doi:10.1029/WR020i007p00944

Cheng, Z., Hsu, T.-J., and Calantoni, J., 2017. SedFoam: a multi-dimensional Eulerian two-phase model for sediment transport and its application to momentary bed failure. *Coastal Engineering*, 119, 32–50. doi:10.1016/j.coastaleng.2016.08.007

Cimorelli, L., *et al*., 2016. A new semi-Lagrangian routing procedure for constituent transport in steady and unsteady flow velocity fields. *Journal of Hydrology*, 538, 216–230. doi:10.1016/j.jhydrol.2016.04.022

Danish Hydraulic Institute, 2007. *Mike 11. A modelling system for rivers and channels*. Hørsholm: User Guide. Danish Hydraulic Institute.

Doherty, J., 2010. Methodologies and software for PEST-based model predictive uncertainty analysis. *Watermark Numerical Computing*, 2010, 1–33.

Drolc, A., and Končan, J.Z., 1996. Water quality modelling of the river Sava, Slovenia. *Water Research*, 30 (11), 2587–2592. doi:10.1016/S0043-1354(96)00154-6

Drolc, A., and Končan, J.Z., 1999. Calibration of QUAL2E model for the Sava river (Slovenia). *Water Science and Technology*, 40 (10), 111–118. doi:10.2166/wst.1999.0509

Duffa, C., *et al*., 2016. Development of emergency response tools for accidental radiological contamination of French coastal areas. *Journal of Environmental Radioactivity*, 151 (2), 487–494. doi:10.1016/j.jenvrad.2015.04.019

Fang, H., *et al*., 2016. Forecasting Yangtze finless porpoise movement behavior using an Eulerian-Eulerian-diffusion method (EEDM). *Ecological Engineering*, 88, 39–52. doi:10.1016/j.ecoleng.2015.12.008

Fletcher, S.J., 2020. Chapter 15 - Applications of semi-Lagrangian methods in the geosciences. *In:* S.J. Fletcher, ed. *Semi-Lagrangian advection methods and their applications in Geoscience*. Amsterdam: Elsevier, 569–593.

Goode, D.J., 1990. Particle velocity interpolation in block-centered finite difference groundwater flow models. *Water Resources Research*, 26 (85), 925–940.

Ho, L., *et al*., 2020. Water research in support of the sustainable Development Goal 6: a case study in Belgium. *Journal of Cleaner Production*, 277, 124082. doi:10.1016/j.jclepro.2020.124082

Holly, F. M., and Preissmann, A., 1977. Accurate calculation of transport in two dimensions. *Journal of the Hydraulics Division*, 103 (11), 1259–1277. doi:10.1061/JYCEAJ.0004870

Jobson, H.E., 1981. Temperature and solute-transport simulation in stream flow using a Lagrangian reference frame: U.S. Geological Survey Water-Resources Investigations Report 81-2. 165.

Jobson, H.E., and Schoelhammer, D.H., 1987. Users manual for a branched Lagrangian transport model: U.S. Geological Survey Water-Resources Investigations Report 87 4163. 73.

Kvočka, D., Žagar, D., and Banovec, P., 2021. A review of river oil spill modeling. *Water*, 13 (12), 1620. doi:10.3390/w13121620.

Little, K.W., and Williams, R.E., 1992. Least-squares calibration of QUAL2E. *Water Environment Research*, 64 (2), 179–185. doi:10.2175/WER.64.2.12

Manson, J.R., *et al*., 2010. A massively parallel semi-Lagrangian algorithm for solving the transport equation. *Procedia Computer Science*, 1 (1), 327–335. doi:10.1016/j.procs.2010.04.036

Manson, J. R., and Wallis, S.G., 2000. A conservative, semi-Lagrangian fate and transport model for fluvial systems"I. Theoretical development. *Water Research*, 34 (15), 3769–3777. doi:10.1016/S0043-1354(00)00131-7

McIntosh, B.S., *et al*., 2011. Environmental decision support systems (EDSS) development – challenges and best practices. *Environmental Modelling & Software*, 26 (12), 1389–1402. doi:10.1016/j.envsoft.2011.09.009

Melching, C.S., and Flores, H.E., 1999. Reaeration equations derived from U.S. *Geological Survey Database. Journal Environmental Engineering*, 125 (5), 407–414.

Mraz, A, *et al*., 2021. Why pathogens matter for meeting the United Nations' sustainable development goal 6 on safely managed water and sanitation. *Water Research*, 189, 116591. doi:10.1016/j.watres.2020.116591

Natarajan, H., and Jacobs, G.B., 2020. An explicit semi-Lagrangian, spectral method for solution of Lagrangian transport equations in Eulerian-Lagrangian formulations. *Computers & Fluids*, 207, 104526. doi:10.1016/j.compfluid.2020.104526

Ndong, M., *et al*., 2017. A novel Eulerian approach for modelling cyanobacteria movement: thin layer formation and recurrent risk to drinking water intakes. *Water Research*, 127, 191–203. doi:10.1016/j.watres.2017.10.021

Neelz, S., and Wallis, S.G., 2007. Tracking accuracy of a semi-Lagrangian method for advection–dispersion modelling in rivers. *International Journal for Numerical Methods in Fluids*, 53 (1), 1. doi:10.1002/fld.1239

Ogrinc, N., *et al*., 2008. Sources and transport of carbon and nitrogen in the River Sava watershed, a major tributary of the River Danube. *Applied Geochemistry*, 23, 3685–3698. doi:10.1016/j.apgeochem.2008.09.003

Oliviera, A., and Baptista, A.M., 1995. A comparison of integration and interpolation Eulerian-Lagrangian methods. *International Journal for Numerical Methods in Fluids*, 21, 183–204. doi:10.1002/fld.1650210302

Orlob, G.T., 1982. Introduction. *In:* G.T. Orlob, ed. *Mathematical modeling of water quality*. Chichester: Wiley/IIASA, 1–7.

Puigferrat, A., *et al*., 2021. Semi-Lagrangian formulation for the advection-diffusion-absorption equation. *Computer Methods in Applied Mechanics and Engineering*, 380. doi:10.1016/j.cma.2021.113807

Quinlivan, L., Chapman, D.V., and Sullivan, T., 2020. Validating citizen science monitoring of ambient water quality for the United Nations sustainable development goals. *Science of The Total Environment*, 699, Article 134255. doi:10.1016/j.scitotenv.2019.134255

Ruan, F., and McLaughlin, D., 1999. An investigation of Eulerian-Lagrangian Methods for solving heterogeneous advection-dominated transport problems. *Water Resources Research*, 35 (8), 2359–2373. doi:10.1029/1999WR900049

Schoellhamer, D.H., 1988. Lagrangian transport modeling with QUAL II kinetics. *Journal of Environmental Engineering*, 114 (2), 368–381. doi:10.1061/(ASCE)0733-9372(1988)114:2(368)

Sir William Halcrow & Partners Ltd. and HR Wallingford Ltd, 2002. ISIS flow user manual. Version 2.1. Sir William Halcrow & Partners Ltd. and HR Wallingford Ltd., Wallingford, U.K.

Sulis, A., and Loucks, D.P., 2007. *Swq model: documentation and user's manual, school of civil and environmental engineering*. Ithaca, NY: Cornell university. 14853 USA.

Thomann, R.V., and Mueller, J.A., 1987. *Principles of surface water quality modeling and control*. New York: Harper-Collins. 644.

Tsani, S., Koundourim, P., and Akinsete, E., 2020. Resource management and sustainable development: a review of the European

water policies in accordance with the United Nations' Sustainable Development Goals. *Environmental Science & Policy*, 114, 570–579. doi:10.1016/j.envsci.2020.09.008

Tsivoglou, E.C., and Neal, L.A., 1976. Tracer measurements of reaeration: III: predicting the reaeration capacity of inland streams. *Journal of Water Pollution Control Federation*, 48 (12), 2669–2689.

UNESCO, UN-Water, 2020. *United nations world water development report 2020: water and climate change*. Paris: UNESCO.

Wang, B., Zhao, G., and Fringer, O.B., 2011. Reconstruction of vector fields for semi-Lagrangian advection on unstructured, staggered grids. *Ocean Modelling*, 40 (1), 52–71. doi:10.1016/j.ocemod.2011.06.003

Wild, T. B., 2011. *Development and evaluation of the stream water quality (SWQ) model*. Doctoral dissertation, Cornell University, School of Civil and Environmental Engineering.

Wild, T. B., and Loucks, D. P., 2012. Development and evaluation of a semi-Lagrangian stream water quality (SWQ) model. *In World Environmental and Water Resources Congress 2012: Crossing Boundaries*, 2283–2293. doi:10.1061/9780784412312.230

Yearsley, J.R., 2009. A semi-Lagrangian water temperature model for advection-dominated river systems. *Water Resouces Research*, 45, W12405.

Yeh, G.-T., 1990. A Lagrangian-Eulerian Method with zoomable hidden fine-mesh approach to solving advection-dispersion equations. *Water Resources Research*, 26 (6), 1133–1144. doi:10.1029/WR026i006p01133

Yeh, G.-T., Chang, J.-R., and Short, T., 1992. An exact peak capturing and oscillation-free scheme to solve advection-dispersion transport equations. *Water Resources Research*, 28, 1133–1144. doi:10.1029/92WR01751

Yosefipoor, P., *et al*., 2022. An adaptive surrogate-based, multi-pollutant, and multi-objective optimization for river-reservoir system management. *Ecological Engineering*, 175, 106487. doi:10.1016/j.ecoleng.2021.106487

Young, D.L., Wang, Y.F., and Eldho, T.I., 2000. Solution of the advection–diffusion equation using the Eulerian–Lagrangian boundary element method. *Engineering Analysis with Boundary Elements*, 24 (6), 449–457. doi:10.1016/S0955-7997(00)00026-6

Zakharov, D.S., and Bansmer, S., 2021. Finite-volume Eulerian solver for simulation of particle-laden flows for icing applications. *Computers & Fluids*, 228, 105009. doi:10.1016/j.compfluid.2021.105009

Zhang, R., Huang, K., and van Genuchten, M.T., 1993. An efficient Eulerian-Lagrangian method for solving solute transport problems in steady and transient flow fields. *Water Resources Research*, 29 (12), 4131–4138. doi:10.1029/93WR01674